Computing accurate bond dissociation energies of emerging per- and polyfluoroalkyl substances: Achieving chemical accuracy using connectivity-based hierarchy schemes

Samir Kumar Nayak,[1,2] and Sharma S. R. K. C. Yamijala[1,2,3,4,*]

1. Department of Chemistry, Indian Institute of Technology Madras, Chennai, 600036 India.
2. Centre for Atomistic Modelling and Materials Design, Indian Institute of Technology Madras, Chennai 600036, India.
3. Centre for Molecular Materials and Functions, Indian Institute of Technology Madras, Chennai 600036, India.
4. Centre for Quantum Information, Communication, and Computing, Indian Institute of Technology Madras, Chennai 600036, India.
* yamijala@iitm.ac.in

Abstract

Understanding the bond dissociation energies (BDEs) of per- and polyfluoroalkyl substances (PFAS) bonds helps in devising their efficient degradation pathways. However, there is only limited experimental data on the PFAS BDEs, and there are uncertainties associated with the BDEs computed using density functional theory. Although quantum chemical methods like the G4 composite method can provide highly accurate BDEs (< 1 kcal mol^{-1}), they are limited to small system sizes. To address DFT's accuracy limitations and G4's system size constraints, we examined the connectivity-based hierarchy (CBH) scheme and found that it can provide BDEs that are reasonably close to the G4 accuracy while retaining the computational efficiency of DFT. To further improve the accuracy, we modified the CBH scheme and demonstrated that BDEs calculated using it have a mean-absolute deviation of 0.7 kcal mol^{-1} from G4 BDEs. To validate the reliability of this new scheme, we computed the ground state free energies of seven PFAS compounds and BDEs for 44 C–C and C–F bonds at the G4 level of theory. Our results suggest that the modified CBH scheme can accurately compute the BDEs of both small and large PFAS at near G4 level accuracy, offering promise for more effective PFAS degradation strategies.

Environmental implication

Effective PFAS mitigation demands advanced degradation strategies. The complete degradation of PFAS includes the dissociation of several C–C and C–F bonds, whose bond dissociation energies (BDEs) change with the surrounding chemical environment. However, the experimental BDEs for most PFAS bonds are unavailable, and are even hard to obtain. Our method achieves near-chemical accuracy in BDEs at DFT cost, facilitating routine studies on diverse PFAS in both gas and solution phases. Using accurate BDEs, feasible degradation mechanisms for all classes of PFAS compounds can be obtained. Therefore, our study offers a crucial tool for comprehensive environmental remediation efforts.

Keywords

PFAS, Connectivity-based hierarchy methods, Bond dissociation energies, accuracy, degradation.

Introduction

Per- and poly-fluoroalkyl substances (PFAS) are man-made pollutants that are ubiquitous in the environment. Due to the presence of strong C–F bonds, these chemicals have widespread usage in various industries such as semiconductors, clothing, non-stick cookware, automotive, and aviation industries.[1–4] At the same time, the presence of C–F bonds makes PFAS environmentally persistent. Moreover, since these chemicals are anthropogenic, biological enzymes are not evolved to degrade them naturally. Consequently, consumption of PFAS-contaminated drinking water will lead to the accumulation of PFAS in living organisms, including humans.[2–5] Toxicological data provides evidence for their presence in various organs of the human body, leading to many pathological diseases, including cancer.[5] Although advanced oxidation and reduction processes are able to degrade these pollutants to some extent, complete degradation is rarely observed.[6–9] Therefore, it is crucial to invent novel PFAS degradation strategies to maintain a safe environment.

It is well-known that the knowledge of bond dissociation energies (BDEs) is crucial in identifying the dominant pathways in combustion, organic synthesis planning, polymer degradation, and drug metabolism.[10–17] Similarly, for designing novel degradation strategies of PFAS, understanding the BDEs of various PFAS bonds is essential. The complete degradation of PFAS includes the dissociation of several C–C and C–F bonds, whose BDEs change with the surrounding chemical environment. Therefore, it is crucial to understand the BDEs of C–C and C–F bonds in various PFAS, for their efficient degradation. Despite their importance, except for a few cases, the experimental BDE values for most of the PFAS bonds are unavailable, and they are even hard to obtain.[18,19] For these reasons, in this work, we aim to obtain accurate BDEs of various PFAS bonds using first-principle calculations.

In general, the BDE of a bond is obtained by computing the differences in the ground state free energies (GSFEs) of the dissociated fragments and the original molecule (i.e., the free energy of the products minus the reactants). The generally accepted procedure to calculate the BDEs includes employing density functional theory (DFT) with a reasonable functional and basis set. However, the major problem with such an approach is that the calculated BDEs vary with both functional and basis sets. In fact, the differences in the predicted BDEs can go as high as 20 kcal mol^{-1}, questioning the reliability of such numbers.[20–22] To circumvent the accuracy issues of DFT, "quantum chemistry composite methods" like G4[23] or correlation consistent composite approach (ccCA)[24] can be employed. These methods are benchmarked against the existing thermodynamic data and are known to provide accurate BDEs with near chemical accuracy (< 1 kcal mol^{-1}). However, the issue with these composite methods is that they need substantial computational resources and cannot be used to study even molecules of moderate sizes (~ 50-100 atoms). To alleviate the problems with both DFT and composite methods, several fragment-based approaches were proposed,[25–29] where accurate ground-state energies of parent molecules are estimated based on the accurate energies of the individual fragments comprising the molecule.

Among the fragment-based approaches, the connectivity-based hierarchy (CBH) approach,[28] developed by Raghavachari's group, has acquired significant attention due to its ability to deliver remarkable accuracy in calculating several thermodynamic properties.[12,30–32] Briefly, in the CBH scheme, the large molecule is divided into several small fragments, and their ground state free energies (GSFEs) are computed at both the DFT and G4 levels of theories. The difference in these energies is considered as the correlation energy of the fragment. The accurate GSFE of a large molecule (for which the G4 calculations are prohibitive) is estimated by summing the "GSFE obtained using DFT" and the "correlation energies of all fragments" (see **Equation 1**). Notably, the accuracy of the GSFE estimated in this manner is dependent on the level of fragmentation, also known as the CBH rung, where a higher rung generally yields better accuracy since it retains the exact hybridization at all heavy atom centers (additional details of the CBH rungs are given in the *methodology* section). It is important to note that while using the CBH scheme, the valency of the generated fragments is satisfied with hydrogen atoms. Here, the original authors used hydrogen atoms since they were mainly focusing on hydrocarbons. However, in PFAS, the majority of the C–H bonds are replaced with the C–F bonds (see **Figure 1**). Therefore, it might be beneficial to satisfy the valence of the carbon atoms of the PFAS fragments with the fluorine atoms instead of the hydrogen atoms. Moreover, such a modification also helps to preserve the chemical environment of the parent PFAS molecule to a larger extent. We call this new scheme where the fluorine atoms are *not* considered as heavy atoms as the "*modified* CBH (mCBH) scheme." Similar to the CBH scheme, the accuracy of the GSFE estimated using the mCBH scheme also depends on the level of fragmentation (mCBH rungs). Since both the CBH and mCBH schemes can be used to calculate the GSFEs of large molecules, in this work, we evaluated the potential of these schemes in determining the GSFEs and BDEs for a range of PFAS molecules.
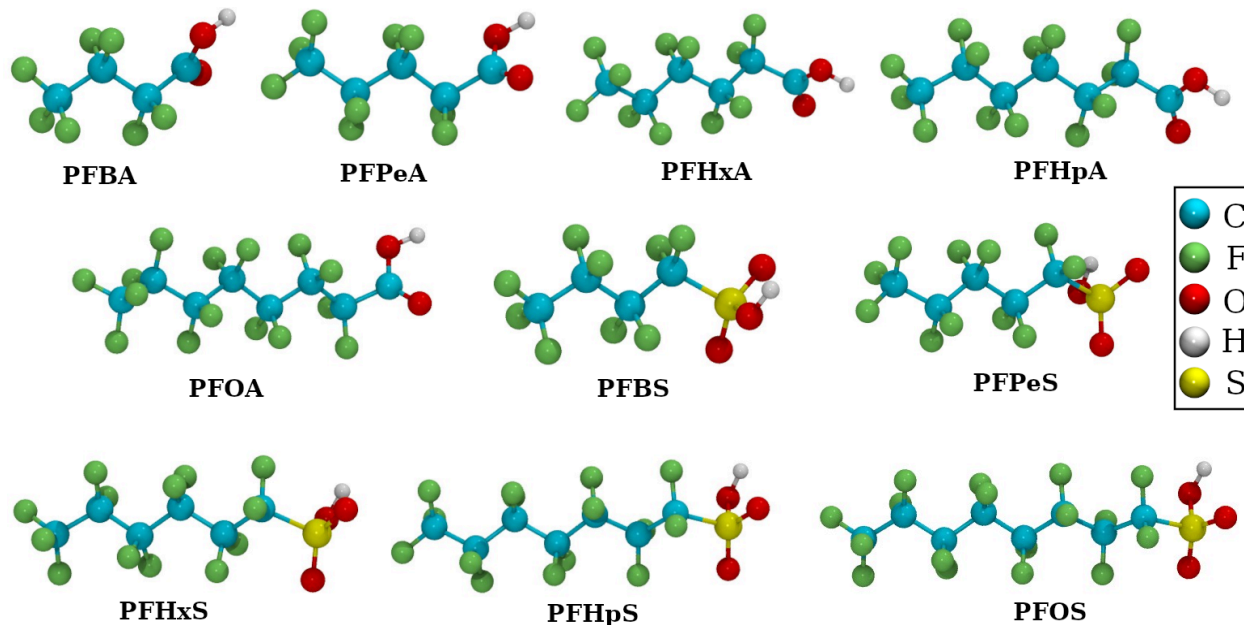

Figure 1: Optimized geometries of perfluorobutanoic acid (PFBA), perfluoropentanoic acid (PFPeA), perfluorohexanoic acid (PFHxA), perfluoroheptanoic acid (PFHpA), perfluorooctanoic acid (PFOA), perfluorobutanesulfonic Acid (PFBS), perfluoropentanesulfonic Acid (PFPeS), perfluorohexanesulfonic

Acid (PFHxS), perfluoroheptanesulfonic Acid (PFHpS), and perfluorooctanesulfonic Acid (PFOS). All the geometries were optimized at the B3LYP/6-31G(2df,p) level of theory.

To assess the accuracy of these schemes, we compared the GSFEs computed using both CBH and mCBH schemes with those obtained at the G4 level of theory across ten representative PFAS molecules (see **Figure 1** and **Table S1**). Of these, five (PFBA, PFPeA, PFHxA, PFHpA, and PFOA) are perfluorocarboxylic acids (PFCAs), and the other five (PFBS, PFPeS, PFHxS, PFHpS, and PFOS) are perfluorosulfonic acids (PFSAs), with carbon chain lengths varying between four to eight. Further, while using the CBH and mCBH schemes, we considered four different exchange-correlation functionals, namely, PBE, B3LYP, M062X, and BHandHLYP. For examining the BDEs' accuracy, we considered 46 bonds within these PFAS molecules and compared the BDEs calculated using the CBH and mCBH schemes with those derived from the G4-level theory. Based on our results, we will show that when combined with M062X or B3LYP functionals, the mCBH scheme can yield GSFEs and BDEs that closely align with their G4 counterparts, with mean absolute deviations less than 1 kcal mol^{-1}.

Methodology

The connectivity-based hierarchy scheme is a chemically intuitive approach for estimating accurate GSFEs of large molecules without performing computationally intensive calculations using the G4 method.[28] For a complete overview of the scheme and its applications, please read the articles by Raghavachari and co-workers.[12,30–32] Below we briefly described this scheme to enable the reader to compute the GSFEs and BDEs of any PFAS molecule, i.e., other than the ones considered in this study. The scheme essentially consists of three steps: (a) First, the ground state free energy of the full molecule is calculated using DFT, $E_{DFT}(full)$. As noted earlier, the E_{DFT}(full) is not completely accurate since DFT does not include all the necessary correlations. (b) Next, the correlation energy is estimated. For this, the large molecule is divided into smaller fragments, and their energies are computed using both G4 and DFT methods, here represented as $E_{G4}(i)$ and $E_{DFT}(i)$, with 'i' being the fragment index. Since the large molecule is fragmented into smaller pieces, performing high-level theory calculations on these fragments is feasible. Moreover, since the energies of each fragment at both G4 and DFT levels are known, we can easily calculate the correlation energy for each fragment, which is simply the difference between the G4 and DFT energies, i.e., $E_{G4}(i) − E_{DFT}(i)$. Next, the total correlation energy (ΔCBH_{corr}) is estimated as the sum of the correlation energies of individual fragments. (c) Finally, the total correlation energy is added to the DFT-calculated energy to estimate the energy of the large molecule at the G4 level of theory, $E_{G4}(full)$. Mathematically,

$$E_{G4}(full) \ − \ E_{DFT}(full) \ \approx \ \sum_i E_{G4}(i) \ − \ \sum_i E_{DFT}(i) \ = \ \Delta CBH_{corr}$$

$$\Rightarrow E_{G4}(full) \ \approx E_{DFT}(full) + \ \Delta CBH_{corr} \qquad\qquad (1)$$

The accuracy of the $E_{G4}(full)$ calculated using the above approach depends on the level of fragmentation, i.e., whether we fragment the entire molecule into simple atoms or bonds or an atom and its immediate neighbors or a bond and its immediate neighbors, and so on. These different fragmentation

4

schemes are often termed different rungs of the CBH scheme and are named CBH-0, CBH-1, etc. Generally, higher rungs provide better accuracies due to the retention of the exact chemical environment at the atomic centers. In a recent work on biodiesel methyl esters,[12] it has been demonstrated that the BDEs obtained at the CBH-2 rung show a mean absolute deviation of about 1.3-1.5 kcal mol^{-1}, and when using CBH-3 rung, the deviation goes below 1 kcal mol^{-1}. Considering these results and with the aim of obtaining accurate BDEs, we used the CBH-3 rung in all our calculations. Similarly, while using the mCBH scheme, we used the mCBH-3 rung.

For the sake of completeness, below, we considered the perfluoropentanoic acid (PFPeA) molecule (see **Scheme 1**) as an example and illustrated the process of generating fragments at the CBH-3 and mCBH-3 rungs. The process and the resulting fragments are also illustrated in **Table S2**. We chose PFPeA since it is one the smallest PFAS molecules possessing all the challenges that we generally meet while constructing the CBH/mCBH rungs (for example, the terminal moiety cancellation to avoid over-counting and addition of molecules on the reactant side, etc.).[28,30] The same procedure can be extended to construct the fragments of any other PFAS.

Construction of fragments at CBH-3 rung for PFPeA: At this rung, the large molecule is divided into fragments based on the bonds between _heavy_ atoms (non-hydrogen atoms). A fragment is formed by considering the "bond-forming" heavy atoms and their immediate heavy atomic neighbors. The inclusion of immediate neighbors ensures that the atomic environment of the parent molecule is largely preserved. Furthermore, to maintain the correct valency, an appropriate number of hydrogen atoms are added to the generated fragments. Below, we illustrated these steps for generating the CBH-3 fragments of the PFPeA molecule (see **Scheme 1**).
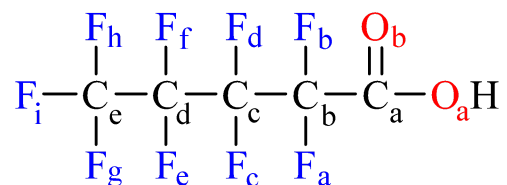
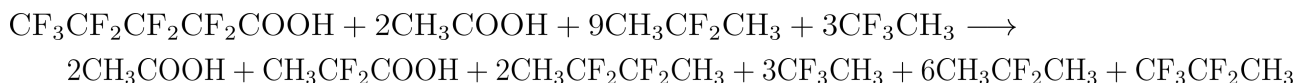**Scheme 1**: Schematic diagram of perfluoropentanoic acid (PFPeA)

First, note that PFPeA contains one C–O, one C꞊O, four C–C (C_a–C_b, C_b–C_c, C_c–C_d, and C_d–C_e), and nine C–F (C_b–F_a/F_b, C_c–F_c/F_d, C_d–F_e/F_f, and C_e–F_h/F_g/F_i,) _heavy_ atomic bonds. Let us start with the C_a–O_a bond. For this bond, the immediate heavy atom neighbors of the "C_a" atom are C_b, O_b, and O_a, and the "O_a" atom does not have any heavy atom neighbors apart from C_a (the other bond is with H). As such, before satisfying the valence, the complete fragment that we should consider at the CBH-3 rung for the C_a–O_a bond is –C_b–(O_b)**C_a**–**O_a**H, where we included all the heavy atom neighbors of the C_a–O_a bond. After satisfying the valence, the fragment becomes H_3C_b–(O_b)**C_a**–**O_a**H, or simply CH_3–COOH. Similarly, the C_a꞊O_b bond also yields CH_3–COOH as its CBH-3 fragment.

Next, let us consider the C_a–C_b bond. For this bond, the immediate heavy atom neighbors of "C_a" are C_b, O_b, and O_a, and for "C_b," they are C_a, C_c, F_a, and F_b. Therefore, the corresponding CBH-3 fragment of the
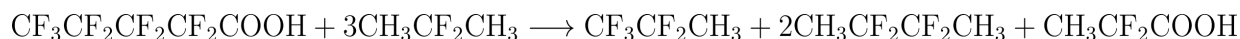
C_a–C_b bond is H_3C_c–$(F_aF_b)C_b$–$C_a(O_b)$–O_aH, or simply CH_3–CF_2–$COOH$. Using the similar arguments, the fragments of C_d–C_c, F_i–C_e, and F_f–C_d bonds are CH_3-CF_2-CF_2-CH_3, CF_3–CH_3, and CH_3–CF_2–CH_3, respectively (more specifically, H_3C_e–$(F_eF_f)C_d$–$C_c(F_cF_d)$–C_bH_3, F_i–$C_e(F_hF_g)$–C_dH_3, and F_f–$C_d(F_e)(C_eH_3)$–C_cH_3). By considering all the bonds, the PFPeA's CBH-3 fragmentation can be summarized in a chemical equation as:

$$CF_3CF_2CF_2CF_2COOH \longrightarrow$$
$$2CH_3COOH + CH_3CF_2COOH + 2CH_3CF_2CF_2CH_3 + 3CF_3CH_3 + 6CH_3CF_2CH_3 + CF_3CF_2CH_3$$

It is important to note that the above equation is not chemically balanced. As explained below, the reason for this imbalance is due to the overcounting of certain units of the PFPeA molecule during the fragmentation. Since CBH-3 is a bond-centric scheme, the atomic environment that is present at the intersection of bonds is naturally repeated in all the bonds. For example, the atomic environment around the C_a (shown in bold) is repeated three times when generating the fragments for the C_a–O_a, C_a=O_b, and C_a–C_b bonds: H_3C_b–$(O_b)C_a$–O_aH, H_3C_b–$(HO_a)C_a$=O_b, and H_3C_c–$(F_aF_b)C_b$–$C_a(O_b)$–O_aH. Although the atomic environment is repeated thrice in the fragments, it is only present once in the parent molecule. To account for this repetition, we need to add fragments corresponding to the repeated parts (with satisfied valency) on the reactant side. In this case, since the –C_b–$C_a(O_b)$–O_aH is repeated thrice, we need to add two CH_3-$COOH$ fragments on the reactants side. Similarly, the atomic environment around the C_b is repeated four times, of which only one time is there in the original molecule. As such, to compensate for the repetition, we need to add three CH_3-CF_2-CH_3 fragments on the reactant side. By proceeding in a similar manner for other atomic centers, we will achieve the following balanced equation,

$$CF_3CF_2CF_2CF_2COOH + 2CH_3COOH + 9CH_3CF_2CH_3 + 3CF_3CH_3 \longrightarrow$$
$$2CH_3COOH + CH_3CF_2COOH + 2CH_3CF_2CF_2CH_3 + 3CF_3CH_3 + 6CH_3CF_2CH_3 + CF_3CF_2CH_3$$

which after rearrangement gives:

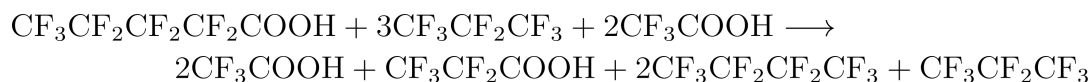$$CF_3CF_2CF_2CF_2COOH + 3CH_3CF_2CH_3 \longrightarrow CF_3CF_2CH_3 + 2CH_3CF_2CF_2CH_3 + CH_3CF_2COOH$$

For all these fragments (both on the left and right sides of the above equation), we can compute the GSFE at both the G4 (E_{G4}) and DFT (E_{DFT}) levels of theory. Further, we can estimate each fragment's correlation energy (missing in DFT) by subtracting the E_{DFT} from the E_{G4}. Finally, by computing the GSFE of the PFPeA molecule using DFT, we can estimate its GSFE at the G4 level using **equation 1**, where the above-computed correlation energies are added to the DFT energy.

Construction of fragments at mCBH-3 rung for PFPeA: As discussed earlier, PFAS compounds have a large number of fluorine atoms, and in the mCBH scheme, the fluorine atoms are not considered as heavy atoms, and they are used to satisfy the valency of the carbon atoms during fragmentation (instead of hydrogens). Please note that we still used hydrogen to satisfy the valency of other heavy atoms like O and S. Again, this helps in preserving the parent molecule's chemical environment to a large extent. Considering this modification into account, the procedure for generating the fragments of PFPeA at the mCBH-3 rung would be as follows: First, since fluorine is no longer considered a heavy atom, we only have three sets of heavy atomic bonds, namely, four C–C, one C–O, and one C=O. The corresponding fragments for the C–O and C

$=O$ bonds, along with their heavy atom neighbors, before satisfying the valency are: $-C_b-(O_b)\mathbf{C_a}-\mathbf{O_a}H$ and $-C_b-(HO_a)\mathbf{C_a}=\mathbf{O_b}$, respectively. After satisfying the valency with fluorine atoms, these fragments become CF_3-COOH. Similarly, the fragment corresponding to the C_a-C_b bond is $F_3C_c-F_2\mathbf{C_b}-\mathbf{C_a}(O_b)-O_aH$, or simply CF_3-CF_2-COOH. Note that we did not specify the indices of F-atoms since they are no more heavy atoms in this scheme. On similar grounds, the fragments corresponding to the C_c-C_b, C_d-C_c, and C_e-C_c bonds are $CF_3CF_2CF_2CF_3$, $CF_3CF_2CF_2CF_3$, and $CF_3CF_2CF_3$, respectively. Therefore, the fragmentation of PFPA at mCBH-3 rung (before balancing) can be summarized as:

$$CF_3CF_2CF_2CF_2COOH \longrightarrow$$
$$2CF_3COOH + CF_3CF_2COOH + 2CF_3CF_2CF_2CF_3 + CF_3CF_2CF_3$$

Similar to the CBH-3 scheme, here also, we need to account for repetition of certain units of the parent molecule in the fragments, and accordingly, the repeated portions have to be added as fragments to the reactant side to balance the chemical equation. Using the arguments we provided in the CBH-3 scheme, the atomic environment around "C_a" is repeated thrice, of which only one time is there in the parent molecule. Accordingly, we need to add two CF_3-COOH molecules to the reactants side to account for the repetition. For the C_b, C_c, and C_d atoms, the atomic environment is repeated only twice (this is because for each of these carbon atoms, there are only two heavy atom carbon neighbors. Remember that fluorines are no longer considered as heavy atoms). Therefore, we have to add one $CF_3-CF_2-CF_3$ molecule to the reactants side for each of these atoms (total 3). For the C_e atom, there is no repetition, and we do not have to add anything to the reactants side. Accordingly, the balanced chemical equation is:

$$CF_3CF_2CF_2CF_2COOH + 3CF_3CF_2CF_3 + 2CF_3COOH \longrightarrow$$
$$2CF_3COOH + CF_3CF_2COOH + 2CF_3CF_2CF_2CF_3 + CF_3CF_2CF_3$$

After canceling the common fragments from both the reactant and product sides, we have

$$CF_3CF_2CF_2CF_2COOH + 2CF_3CF_2CF_3 \longrightarrow 2CF_3CF_2CF_2CF_3 + CF_3CF_2COOH$$
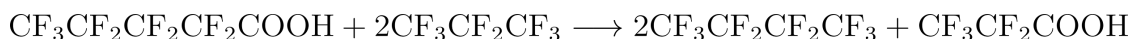
Once again, by computing the correlation energies of each of these mCBH-3 fragments and by knowing PFPeA's GSFE at the DFT level, we can estimate its GSFE at the G4 level using **equation 1**. In general, if we only want to estimate the GSFE of a PFAS molecule at the G4 level, then performing a DFT calculation for the parent molecule (here, PFPeA) is sufficient. However, if we want to evaluate the accuracy of these schemes, we also need to compute the GSFE of the parent molecule at the G4 level (which is a computationally demanding task).

Similar calculations need to be performed for computing the BDEs, where the GSFEs of both the parent molecule and the dissociated fragments need to be computed either at the CBH-3/mCBH-3 schemes (if we only want to estimate the BDE) or at the G4 level (if we want to evaluate the accuracy of the BDEs obtained using the CBH-3/mCBH-3 schemes). The fragment generation procedure for computing the BDEs of various PFPeA bonds is illustrated in the supporting information (after **Scheme S2**).

Computational details

All electronic structure calculations were performed using the Gaussian 09[33] suite of programs (unfortunately, the G16 Rev B.01 version gives incorrect G4 energies).[34] For optimizing the PFAS molecules, we considered the 6-31G(2df,p) basis set and employed four widely-used exchange-correlation functionals, namely, B3LYP,[35] M062X,[36] BHandHLYP,[37] and PBE.[38] Here, we chose the 6-31G(2df,p) basis set since the same basis set is used for optimizing molecules within the G4 composite method. For the optimized geometries, we conducted the frequency calculations and did not observe any imaginary frequencies, proving that these geometries are at a minimum of the ground-state potential energy surface. Next, these geometries were used to compute the Gibbs free energies of PFAS at 298.15 K. The free energy data was further used to compute the Gibbs energy of bond dissociation (hereafter, simply referred to as bond dissociation energies, BDEs) for various bonds in each of the PFAS molecules. It should be noted that we reported both ground-state free energies (GSFEs) and BDEs at different levels of theory, such as plain DFT, the composite G4 method, and the G4-corrected DFT results through CBH-3/mCBH-3 schemes (hereafter, simply referred to as CBH-3/mCBH-3 schemes). The level of theory that we are referring to will be clear based on the context.

Results and Discussion

We first computed the ground state free energies of ten PFAS molecules at both the G4 level of theory and using the CBH-3 and mCBH-3 schemes. In **Figure 3**, we presented the mean absolute deviation (MAD) in the CBH-3 and mCBH-3 GSFEs from the G4 GSFEs. It is important to note that the G4 calculations are computationally quite demanding, and some of them did not converge even after two months (see **Tables S3 and S4** for more information). Among the ten molecules, we could only compute the GSFEs of seven molecules, namely PFBA, PFPeA, PFHxA, PFHpA, PFOA, PFBS, and PFPeS, at the G4 level of theory. As such, although the CBH-3/mCBH-3 results are available for all ten PFAS molecules, we presented the differences between the G4 and CBH-3/mCBH-3 results only for the seven molecules mentioned above.
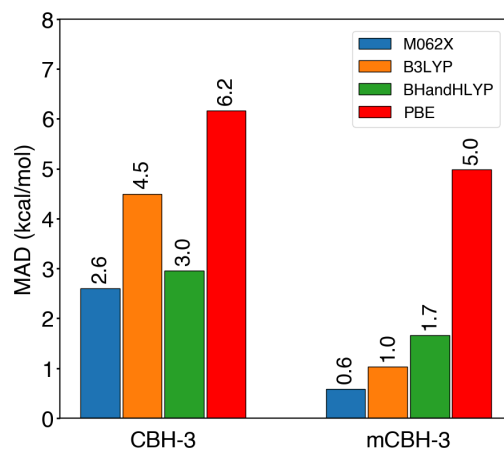
Figure 2. The difference between the ground-state free energies calculated using either the CBH-3 or mCBH-3 schemes and the G4 level of theory. The CBH-3 and mCBH-3 schemes were employed along with four different exchange-correlation functionals. The mean absolute deviations (MAD) are shown for all these functionals. Seven molecules, namely, PFBA, PFPeA, PFHxA, PFHpA, PFOA, PFBS, and PFPeS, are considered in these calculations.

As shown in **Figure 2**, the GSFEs calculated using the CBH-3 and mCBH-3 schemes deviate moderately from the G4 predicted values (i.e., MAD values are small). Even when using a non-hybrid functional like PBE, the maximum deviation was only 6.2 kcal mol^{-1}. Further, this deviation has reduced to as low as 0.6 kcal mol^{-1} when using a hybrid functional like M062X in conjunction with the mCBH-3 scheme. *Apparently, these results indicate that employing the CBH-3/mCBH-3 schemes helps to obtain GSFEs that are as accurate as the G4 predicted GSFEs, but only at the DFT cost.* Among the four functionals, M062X gave the most accurate GSFEs when used in conjunction with both the CBH-3 (MAD = 2.6 kcal mol^{-1}) and mCBH-3 (MAD = 0.6 kcal mol^{-1}) schemes, and PBE produced the least accurate results. Between CBH-3 and mCBH-3, the mCBH-3 scheme outperformed the CBH-3 scheme in providing accurate GSFEs. *Overall, based on our results, we strongly support using the M062X functional along with the mCBH-3 scheme for obtaining accurate GSFEs of PFAS.*

Next, we examined the efficacy of CBH-3 and mCBH-3 schemes in predicting the BDEs of PFAS. Since BDE is calculated by taking the *difference* between the GSFEs of the parent and fragmented molecules, it is often assumed that the errors associated with the absolute values of the GSFEs would cancel with each other while taking the differences, thereby producing accurate BDEs. Indeed, this assumption holds true for some cases and serves as the basis for the widespread usage of DFT functionals in BDE calculations.[32,39] However, this assumption is *not* universally applicable. For example, in a recent study on PFAS, Paultre et al. showed that the bond dissociation energies predicted using wB97XD/6-311+G(d,p) and G3 (CC, MP2) differ by ~9.1 kcal mol^{-1}, where the latter method provides accurate results.[43] In another study, Melin et al. showed that the enthalpies of formation of perfluoroalkanes predicted using B3LYP and M062X could differ by as high as 78 kcal mol^{-1}![44] As such, the BDEs computed using DFT functionals are not only error prone, but also significantly differ from functional to functional. Therefore, it is desirable to design a method that provides BDEs that are accurate and agnostic to the functional choice. Below, we show that if DFT functionals are combined with the CBH-3 and mCBH-3 schemes, they can yield consistent and accurate BDEs for PFAS, irrespective of the functional used. Additionally, apart from BDEs, numerous physical properties – such as adsorption energy, binding energy, reaction energy, pKa, and redox potentials – require the calculation of differences in GSFEs rather than their absolute values.[12,32,39–42] Consequently, the accuracy of BDEs obtained using the CBH-3 or mCBH-3 schemes can provide valuable insights into the achievable accuracy for the aforementioned physical properties.

Before proceeding to analyze the BDEs of various C–C and C–F bonds across several PFAS molecules, we would like to focus on one specific PFAS molecule and evaluate the accuracy of CBH-3 and mCBH-3 schemes in predicting the BDEs of all of its bonds. To this end, we considered PFBA (see inset of **Figure 3b**), a small molecule for which the BDEs of all the bonds (C_2–F, C_3–F, C_4–F, C_1–C_2, C_2–C_3, C_3–C_4, C_1–O, and O–H) can be computed at the G4 level of theory within a reasonable computational cost. After computing the BDEs of all PFBA bonds at the G4 level of theory, we compared them against the BDEs obtained using (i) the plain DFT functionals (blue color), (ii) when DFT functionals are used in conjunction with the CBH-3 (orange color), and (iii) mCBH-3 (green color) schemes, as depicted in **Figures 3** and **S1**.

9

Also, the actual BDE values computed at various levels of theory are given in **Table 1**. From these results, it is apparent that *the BDEs predicted using the plain DFT functionals deviate significantly from the G4 BDEs.* For example, for the C_3–F and C_4–F bonds, the DFT BDEs deviate by as high as 10.2 kcal mol^{-1} from the G4 BDEs. Similarly, the BDEs of several C–C bonds deviate by $\sim$ 8 kcal mol^{-1}, and the C–O and O–H bonds deviate by $\sim$ 9 kcal mol^{-1}. As discussed earlier, Paultre et al. showed that the BDEs of C–F and C–C bonds of PFBA computed using wB97XD/6-311+G(d,p) differ from the G3(CC,MP2) BDE values by 9.1 kcal mol^{-1}.[43] As such, apart from the DFT functionals that we considered, other functionals also yield BDEs that deviate largely from the G3 or G4 predicted BDEs (where, G4 is more accurate than G3).

Table 1: The bond dissociation energies of all the C–C, C–F, C–O, and O–H bonds of a PFBA molecule computed at various levels of theory. The deviations from the G4 BDEs are given in parentheses. The bond numbers are according to the IUPAC numbering scheme (for example, see the inset of **Figure 4b**).

| Bond	G4	DFT				CBH-3				mCBH-3			
		M062X	B3LYP	BHand HLYP	PBE	M062X	B3LYP	BHand HLYP	PBE	M062X	B3LYP	BHand HLYP	PBE
C_1-C_2	70.25	76.75 (6.51)	66.51 (3.74)	68.39 (1.86)	68.98 (1.27)	69.85 (0.39)	70.95 (0.71)	70.54 (0.29)	69.59 (0.66)	69.90 (0.34)	70.11 (0.14)	69.83 (0.42)	68.60 (1.65)
C_2–C_3	67.39	72.39 (5.00)	59.72 (7.67)	61.70 (5.69)	61.29 (6.1)	68.91 (1.52)	69.92 (2.53)	69.08 (1.69)	70.77 (3.38)	67.04 (0.35)	67.25 (0.14)	66.98 (0.41)	65.74 (1.65)
C_3–C_4	104.77	109.46 (4.69)	97.57 (7.20)	101.34 (3.43)	99.34 (5.43)	106.72 (1.95)	107.00 (2.23)	106.62 (1.85)	107.21 (2.44)	104.43 (0.34)	104.64 (0.13)	104.36 (0.41)	103.13 (1.64)
C_2–F	95.96	103.84 (7.88)	97.72 (1.76)	90.66 (5.3)	104.67 (8.71)	96.33 (0.37)	97.25 (1.29)	96.55 (0.59)	96.24 (0.28)	95.69 (0.27)	96.70 (0.74)	96.51 (0.55)	95.39 (0.57)
C_3–F	102.60	112.77 (10.17)	105.70 (3.10)	98.53 (4.07)	112.74 (10.14)	103.57 (0.97)	103.52 (0.92)	102.97 (0.37)	103.50 (0.9)	101.93 (0.67)	102.38 (0.22)	102.01 (0.59)	100.58 (2.02)
C_4–F	110.48	119.98 (9.50)	113.72 (3.24)	106.97 (3.51)	120.68 (10.20)	111.08 (0.60)	110.89 (0.41)	112.13 (1.65)	110.26 (0.22)	110.13 (0.35)	109.86 (0.62)	110.01 (0.47)	109.77 (0.71)
C_1–O	93.76	103.58 (9.82)	95.75 (1.99)	91.78 (1.98)	103.45 (9.69)	94.88 (1.12)	94.81 (1.05)	96.17 (2.41)	94.45 (0.69)	92.53 (1.23)	93.55 (0.21)	93.41 (0.35)	91.97 (1.79)
O–H	100.99	106.51 (5.52)	97.79 (3.20)	100.33 (0.66)	91.87 (9.12)	101.91 (0.92)	103.07 (2.08)	103.11 2.12)	102.78 (1.79)	101.72 (0.73)	101.92 (0.93)	102.00 (1.01)	101.86 (0.87)

10
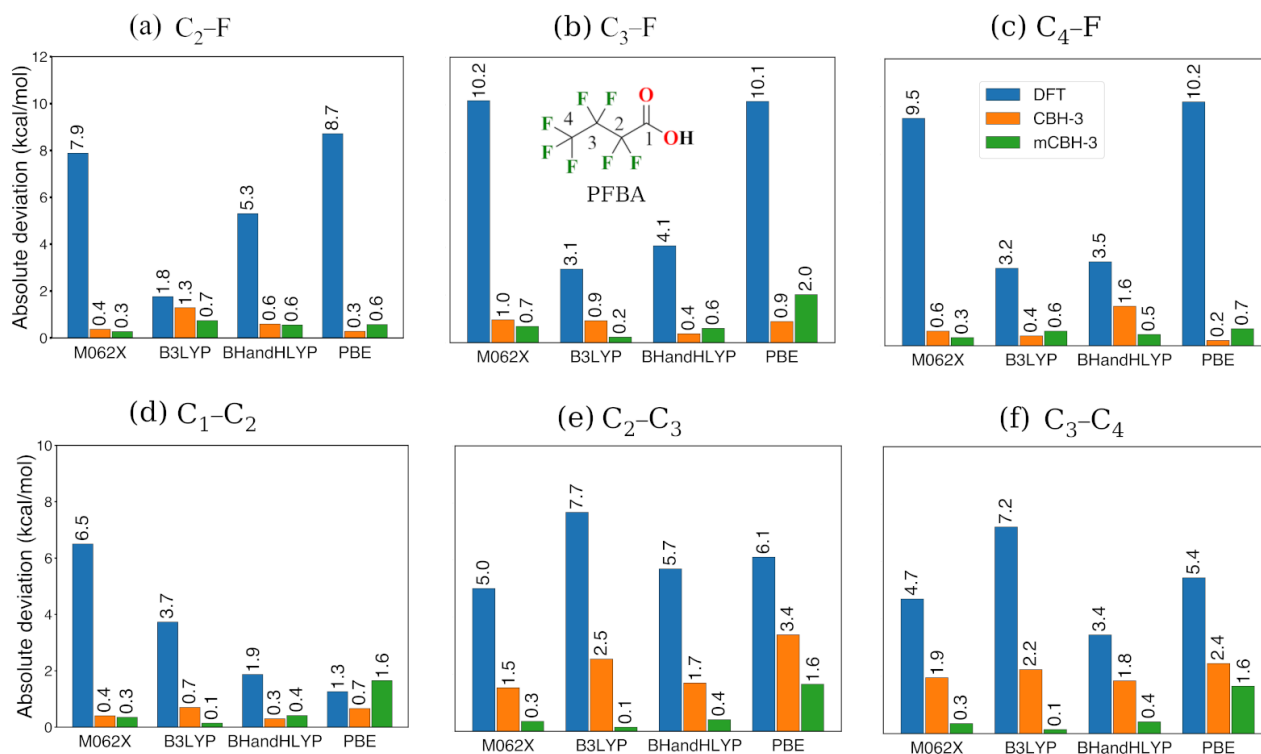
Figure 3. The absolute deviation in the gas-phase BDEs of (a) C_2–F, (b) C_3–F, (c) C_4–F, (d) C_1–C_2, (e) C_2–C_3, and (f) C_3–C_4 bonds of the PFBA molecule. The BDEs of C_1–O and O–H bonds are given in **Figure S1.** Blue, orange, and green colors depict the deviations in the BDEs when calculated using a DFT functional, a DFT functional combined with the CBH-3 scheme, and a DFT functional combined with the mCBH-3 scheme, respectively. Results of four different functionals, namely, M062X, B3LYP, BHandHLYP, and PBE, are shown. All the deviations are with respect to the BDEs predicted at the G4 level of theory. Inset in panel (b) depicts the PFBA molecule and the numbering scheme.

Furthermore, the amount of deviation from the G4 value varies largely from functional to functional. For example, for the C_3–F bond, the BDE value predicted using the M062X functional deviates by 10.2 kcal mol^{-1} from the G4 value, whereas the B3LYP value only deviates by 3.1 kcal mol^{-1}. *Thus, the bond dissociation energy of the same C–F bond predicted using M062X and B3LYP functionals differ by 7.1 kcal mol^{-1}.* Here, we would like to emphasize that one should not interpret the former result as "B3LYP provides more accurate BDEs than the M062X". Indeed, the B3LYP predicted C–C BDEs of the PFBA molecule deviate largely from the G4 values than the M062X predicted BDEs. *As such, these results indicate that although a DFT functional (say, B3LYP) might provide accurate BDEs for certain bonds of a molecule (here, C–F bonds of PFBA), it is not guaranteed that it would provide accurate BDEs for all bonds of the same molecule (here, C–C bonds of PFBA).* In other words, DFT functionals exhibit irregular trends in accuracy across different bonds of the same molecule. Undoubtedly, using different functionals to compute the BDEs of different bonds of the same molecule is undesirable.

Interestingly, the above differences reduce drastically when the DFT calculations are integrated with either the CBH-3 or mCBH-3 schemes. For instance, considering the same C_3–F bond, the deviation in the BDE value predicted using the M062X functional decreases from 10.2 kcal mol^{-1} to 1.0 (0.7) kcal mol^{-1} when the calculation is integrated with the CBH-3 (mCBH-3) scheme, i. e., *a tenfold enhancement in the BDE*

11

accuracy is obtained by utilizing the CBH-3/mCBH-3 schemes, all still at the DFT cost. Moreover, remarkably, the mCBH-3 scheme provides accurate BDEs for all the PFBA bonds, i.e., not just for a specific bond. When integrated with the mCBH-3 scheme, M062X, B3LYP, and BHandHLYP functionals showed a maximum (minimum) absolute deviation of 1.23 kcal mol^{-1} (0.14 kcal mol^{-1}) from the G4 BDEs (see **Table 1**), *indicating that these results are close to the chemical accuracy*. Only PBE functional showed slightly higher deviations; maximum (minimum) deviation is 2.02 kcal mol^{-1} (0.57 kcal mol^{-1}). Considering the semi-local nature of the PBE functional, such a small deviation is acceptable. However, it is noteworthy to mention that the BDEs obtained using the PBE functional in conjunction with CBH-3/mCBH-3 scheme exhibit greater accuracy compared to those obtained through plain DFT functionals, including hybrid and global-hybrid functionals. Therefore, integrating the DFT functionals with CBH-3/mCBH-3 schemes is highly beneficial for obtaining accurate BDEs instead of using the plain DFT functionals. *Furthermore, the BDE of a bond computed using the mCBH-3 scheme is almost the same irrespective of the functional used, which is one of the most desired results!* For example, after integrating with mCBH-3 scheme, the maximum difference in the BDEs of any PFBA bond computed using M062X, B3LYP, and BHandHLYP functionals is less than ~ 1 kcal mol^{-1}. Together, these results strongly establish the validity of using the CBH-3 and mCBH-3 schemes for computing the BDEs of any PFAS molecule.

Motivated by these encouraging findings, we considered a larger data set and conducted a thorough evaluation to assess the accuracy of CBH-3 and mCBH-3 schemes in predicting the BDEs of C–C and C–F bonds. To this end, we computed the BDEs of 46 distinct bonds, spanning across different PFAS molecules. Similar to the approach described earlier, we initially computed these BDEs at the G4 level of theory and then compared them against the results obtained using (i) the plain DFT functionals, and (ii) when DFT functionals are used in tandem with the CBH-3 and mCBH-3 schemes. In these calculations, to reduce the computational cost, we only considered two (instead of four) DFT functionals, namely, M062X and B3LYP. The resulting BDEs for the 28 C–C, 16 C–F, one C–O, and one O–H bonds, computed across all levels of theory, are given in **Table 2**, and the mean absolute deviations (MAD) in the BDEs from the G4 values, for each level of theory, are depicted in **Figure 4**. Moreover, the absolute deviations are also reported in **Table 2**. *It is crucial to note that obtaining experimental BDEs is a challenging task and is limited to small molecules only.[18] Hence, this benchmark against the G4 calculations would be helpful for all the future BDE calculations of different bonds of large PFAS.*
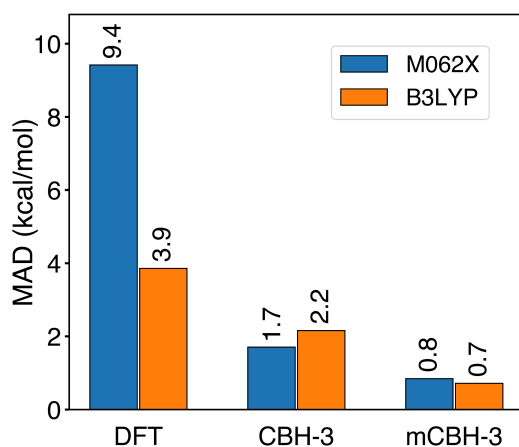
Figure 4. The mean absolute deviation (MAD) in the BDEs from the G4 values. Here, BDEs are computed using the plain DFT functionals (M062X and B3LYP), and when DFT functionals are used in tandem with the CBH-3 and mCBH-3 schemes. For calculating the MAD values, BDEs of 28 C–C bonds, 16 C–F, one C–O, one O–H bonds are considered. For all these bonds, the absolute deviation in the BDEs from the G4 values are provided in **Table 2**.

From **Figure 4**, it can be noticed that the BDEs predicted using plain DFT functionals exhibit significant deviations from the G4 values, with the MAD values of 9.4 and 3.9 kcal mol^{-1} for the M062X and B3LYP functionals, respectively. Among the 46 bonds that we considered in our calculations, the largest deviation in the BDE is observed for the C_6–C_7 bond of PFOA, where the M062X result deviates by 12.7 kcal mol^{-1} from the G4 value (see **Table 2**). Notably, for the same bond, the BDEs computed using M062X and B3LYP functionals differ by ~ 12 kcal mol^{-1}, highlighting the uncertainties associated with the DFT BDEs. However, when the M062X functional is used in conjunction with the CBH-3 and mCBH-3 schemes, the deviation diminishes to 4.33 and 1.34 kcal mol^{-1}, respectively, indicating a remarkable improvement. Similarly, with the B3LYP functional, a maximum absolute deviation of ~ 7.7 kcal mol^{-1} is observed for the C_2–C_3 bond of PFBA, and the deviation reduces to 2.53 and 0.14 kcal mol^{-1}, after integrating the functional with the CBH-3 and mCBH-3 schemes, respectively. Finally, as evident from **Figure 4**, the mCBH-3 scheme consistently outperforms the CBH-3 scheme by yielding BDEs that are significantly close to the G4 values (with MAD values < 1 kcal mol^{-1} for both B3LYP and M062X functionals). *Overall, our simulations suggest that the mCBH-3 scheme in conjunction with M062X or B3LYP functionals can yield BDEs that are as accurate as G4 results (with errors < 1 kcal mol^{-1}).* In other words, when the G4 level of theory cannot be used to compute the BDEs of a PFAS molecule (due to the associated computational cost), it is advisable to use the mCBH-3 scheme.

Table 2: A comparison of the bond dissociation energies obtained using different levels of theory. C–C and C–F bonds of various PFAS are considered in these calculations. The absolute deviation in the bond dissociation energies from the G4 values are given in parentheses. The bond numbering schemes are given according to the IUPAC convention (see **Table S1**). Since the BDEs of all PFBA bonds are given in **Table 1**, we did not repeat them here.

Molecule	Bond	G4	DFT		CBH-3		mCBH-3	
			M062X	**B3LYP**	**M062X**	**B3LYP**	**M062X**	**B3LYP**
PFPeA	C_1–C_2	70.68	77.99 (7.31)	67.50 (3.18)	71.63 (0.95)	71.78 (1.10)	70.11 (0.57)	70.19 (0.49)
	C_2–C_3	64.98	70.61 (5.63)	57.56 (7.42)	65.38 (0.40)	66.82 (1.84)	64.41 (0.57)	64.49 (0.49)
	C_3–C_4	70.30	80.22 (9.92)	67.18 (3.12)	73.04 (2.74)	73.66 (3.36)	69.72 (0.58)	69.81 (0.49)
	C_4–C_5	102.48	107.80 (5.32)	95.65 (6.83)	103.88 (1.40)	104.03 (1.55)	101.91 (0.57)	101.51 (0.97)
	C_2–F	94.73	105.27 (10.54)	97.18 (2.45)	98.30 (3.57)	96.56 (1.83)	96.09 (1.36)	95.26 (0.53)
	C_3–F	100.51	110.95 (10.44)	104.32 (3.81)	99.76 (0.75)	101.21 (0.70)	98.72 (1.79)	100.06 (0.45)
	C_4–F	99.98	111.43 (11.45)	103.64 (3.66)	101.03 (1.05)	100.41 (0.43)	99.72 (0.26)	99.12 (0.86)
	C_5–F	109.53	120.05 (10.52)	113.83 (4.30)	111.15 (1.62)	111.00 (1.47)	110.20 (0.67)	109.98 (0.45)

PFHxA	C_1–C_2	68.40	76.73 (8.33)	66.15 (2.25)	70.38 (1.98)	70.42 (2.02)	68.85 (0.45)	68.83 (0.43)
	C_2–C_3	65.41	71.74 (6.33)	58.40 (7.01)	67.05 (1.64)	67.50 (2.09)	64.51 (0.90)	64.43 (0.98)
	C_3–C_4	67.87	78.32 (10.45)	64.86 (3.01)	69.40 (1.53)	70.42 (2.55)	66.98 (0.89)	66.90 (0.97)
	C_4–C_5	67.99	78.45 (10.46)	65.11 (2.88)	70.09 (2.10)	70.54 (2.55)	67.10 (0.09)	66.54 (1.45)
	C_5–C_6	101.51	107.76 (6.25)	95.62 (5.89)	103.83 (2.32)	103.99 (2.48)	101.86 (0.35)	101.48 (0.03)
	C_2–F	93.35	103.57 (10.22)	96.56 (3.21)	96.61 (3.26)	95.93 (2.58)	94.4 (1.05)	94.64 (1.29)
	C_3–F	99.28	110.7 (11.42)	103.67 (4.39)	100.06 (0.78)	100.39 (1.11)	97.44 (1.84)	98.5 (0.78)
	C_4–F	98.72	109.73 (11.01)	103.16 (4.44)	97.36 (1.36)	98.99 (0.27)	96.64 (2.08)	97.69 (1.03)
	C_5–F	99.35	111.34 (11.99)	103.9 (4.55)	100.95 (1.6)	100.66 (1.31)	99.63 (0.28)	99.37 (0.02)
	C_6–F	108.41	120.19 (11.78)	113.66 (5.25)	111.29 (2.88)	110.83 (2.42)	110.34 (1.93)	109.8 (1.39)
PFHpA	C_2–C_3	63.11	70.41 (7.30)	57.11 (6.00)	65.73 (2.62)	66.20 (3.09)	63.18 (0.07)	63.13 (0.02)
	C_3–C_4	68.29	79.38 (11.09)	65.77 (2.52)	71.00 (2.71)	71.16 (2.87)	67.01 (1.28)	66.90 (1.39)
	C_4–C_5	65.56	76.48 (10.92)	62.85 (2.71)	66.38 (0.82)	67.35 (1.79)	64.28 (1.28)	63.69 (1.87)
	C_5–C_6	67.01	78.34 (11.33)	65.14 (1.87)	69.97 (2.96)	70.57 (3.56)	66.98 (0.03)	66.56 (0.45)
	C_6–C_7	100.38	107.83 (7.45)	95.51 (4.87)	103.91 (3.53)	103.88 (3.5)	101.94 (1.56)	101.37 (0.99)
PFOA	C_3–C_4	66.02	78.25 (12.23)	64.59 (1.43)	69.88 (3.96)	69.98 (3.96)	65.88 (0.14)	65.72 (0.30)
	C_4–C_5	66.00	77.74 (11.74)	63.88 (2.12)	68.17 (2.17)	68.21 (2.21)	64.50 (1.50)	63.80 (2.20)
	C_5–C_6	64.61	76.57 (11.96)	63.00 (1.61)	66.46 (1.85)	67.50 (2.89)	64.36 (0.25)	63.83 (0.78)
	C_6–C_7	65.91	78.61 (12.7)	65.15 (0.76)	70.24 (4.33)	70.58 (4.67)	67.25 (1.34)	66.57 (0.66)
PFBS	C_1–C_2	67.27	76.65 (9.38)	63.61 (3.66)	66.63 (0.64)	68.85 (1.58)	67.68 (0.41)	66.24 (1.03)
	C_2–C_3	67.68	78.08 (10.4)	64.60 (3.08)	69.23 (1.55)	73.48 (5.8)	68.09 (0.41)	66.65 (1.03)
	C_3–C_4	102.01	107.8 (5.79)	95.52 (6.49)	103.27 (1.26)	104.06 (2.05)	104.49 (2.48)	102.49 (0.48)
	C_1–F	97.97	109.59 (11.62)	103.15 (5.18)	98.18 (0.21)	98.72 (0.75)	98.96 (0.99)	96.89 (1.08)
	C_2–F	98.33	109.1 (10.77)	102.07 (3.74)	96.64 (1.69)	101.18 (2.85)	99 (0.67)	98.07 (0.26)
	C_3–F	100.92	111.16 (10.24)	104.15 (3.23)	100.16 (0.76)	101.08 (0.16)	102.04 (1.12)	100.73 (0.19)
	C_4–F	108.92	119.91 (10.99)	113.59 (4.67)	111.01 (2.09)	110.76 (1.84)	110.06 (1.14)	109.73 (0.81)

PFPeS	C_1–C_2	67.66	77.78 (10.12)	64.49 (3.17)	68.29 (0.63)	69.57 (1.91)	67.77 (0.11)	66.21 (1.45)
	C_2–C_3	65.23	76.18 (10.95)	62.32 (2.91)	65.58 (0.35)	70.27 (5.04)	65.33 (0.1)	63.78 (1.45)
	C_3–C_4	67.5	78.44 (10.94)	65.01 (2.49)	69.47 (1.97)	70.61 (3.11)	69.67 (2.17)	67.55 (0.05)
	C_4–C_5	100.88	107.61 (6.73)	95.41 (5.47)	103.69 (2.81)	103.79 (2.91)	101.72 (0.84)	101.27 (0.39)

Conclusions and Outlook

In summary, we demonstrated that the modified connectivity-based hierarchy (mCBH) approach is a powerful scheme to compute the ground state free energies (GSFEs) and bond dissociation energies (BDEs) of PFAS. Specifically, we showed that mCBH could deliver GSFEs and BDEs with accuracy close to the G4 level, while maintaining a computational cost that is comparable to running a DFT calculation. To illustrate the advantages and wide-applicability of the mCBH scheme, we conducted computationally intensive G4 calculations for several molecules, and obtained BDEs of 46 bonds spanning across various PFAS. First, using four widely-used exchange-correlation functionals, we showed that BDEs predicted using the plain DFT functionals deviate significantly (> 12 kcal mol^{-1}) from the G4 BDEs. Also, we consistently find that DFT functionals exhibit irregular trends in accuracy across different bonds of the same molecule. Even more alarmingly, the BDE of the same bond predicted using M062X and B3LYP functionals was found to differ by 12 kcal mol^{-1}! Next, we showed that such large discrepancies in the BDE results can be corrected by integrating the DFT functionals with the mCBH scheme. Specifically, we demonstrated a tenfold enhancement in the BDE accuracy, and established that the computed BDEs are largely independent from the functional choice. Furthermore, we illustrated that even when a semi-local functional like PBE is integrated with the mCBH scheme, it can provide BDEs that are more accurate than the BDEs obtained through plain DFT functionals like B3LYP, M062X, and BHandHLYP. Overall, our simulations suggest that the mCBH scheme in conjunction with DFT functionals, like M062X or B3LYP, can yield BDEs that are as accurate as G4 results, with mean absolute deviations less than 1 kcal mol^{-1}.

Given the challenges associated with obtaining experimental BDEs and their limitation to small molecules,[18] our study with 46 BDEs computed at the G4 level of theory for PFAS of various lengths would be a great benchmark for all the future BDE calculations. Moreover, with the mCBH scheme's ability to obtain BDEs at near chemical accuracy, studying diverse PFAS with varying chain lengths and functional groups in both gas and solution phases can be routinely conducted, and such studies will further help to understand the variation in C–F or C–C bond strengths across diverse PFAS compounds. Finally, with the access to accurate BDEs, feasible degradation mechanisms for all classes of PFAS compounds can be obtained. Some of these avenues are being actively pursued in our group and the results will be communicated elsewhere.

Author contributions

Samir Kumar Nayak: Methodology, Software, Validation, Formal analysis, Investigation, Data curation, Writing – original draft, Writing – review & editing, Visualization; Sharma S.R.K.C. Yamijala: Conceptualization, Methodology, Validation, Formal analysis, Resources, Writing – original draft, Writing – review & editing, Supervision, Project administration, Funding acquisition.

Conflicts of interest

There are no conflicts to declare.

Acknowledgements

References

(1) Manzetti, S.; van der Spoel, E. R.; van der Spoel, D. Chemical Properties, Environmental Fate, and Degradation of Seven Classes of Pollutants. *Chem. Res. Toxicol.* **2014**, *27* (5), 713–737.

(2) Yamijala, S. S. R. K. C.; Shinde, R.; Wong, B. M. Real-Time Degradation Dynamics of Hydrated per- and Polyfluoroalkyl Substances (PFASs) in the Presence of Excess Electrons. *Phys. Chem. Chem. Phys.* **2020**, *22* (13), 6804–6808.

(3) Falandysz, J.; Taniyasu, S.; Gulkowska, A.; Yamashita, N.; Schulte-Oehlmann, U. Is Fish a Major Source of Fluorinated Surfactants and Repellents in Humans Living on the Baltic Coast? *Environ. Sci. Technol.* **2006**, *40* (3), 748–751.

(4) Ameduri, B.; Sawada, H. *Fluorinated Polymers: Volume 1: Synthesis, Properties, Processing and Simulation*; Royal Society of Chemistry, 2016.

(5) Çeçen, F.; Tezel, U. *Hazardous Pollutants in Biological Treatment Systems: Fundamentals and a Guide to Experimental Research*; IWA Publishing, 2017.

(6) Stability of Fluorinated Surfactants in Advanced Oxidation processes—A Follow up of Degradation Products Using Flow Injection–mass Spectrometry, Liquid Chromatography–mass Spectrometry and Liquid Chromatography–multiple Stage Mass Spectrometry. *J. Chromatogr. A* **2005**, *1082* (1), 110–119.

(7) Bentel, M. J.; Yu, Y.; Xu, L.; Li, Z.; Wong, B. M.; Men, Y.; Liu, J. Defluorination of Per- and Polyfluoroalkyl Substances (PFASs) with Hydrated Electrons: Structural Dependence and Implications to PFAS Remediation and Management. *Environ. Sci. Technol.* **2019**, *53* (7), 3718–3728.

(8) Photodegradation of per- and Polyfluoroalkyl Substances in Water: A Review of Fundamentals and Applications. *J. Hazard. Mater.* **2022**, *439*, 129580.

(9) A Review of Emerging Photoinduced Degradation Methods for per- and Polyfluoroalkyl Substances in Water. *Curr. Opin. Chem. Eng.* **2023**, *41*, 100947.

(10) O'Reilly, R. J.; Karton, A.; Radom, L. Effect of Substituents on the Strength of N-X (X = H, F, and Cl) Bond Dissociation Energies: A High-Level Quantum Chemical Study. *J. Phys. Chem. A* **2011**, *115* (21), 5496–5504.

(11) Akbar Ali, M.; Violi, A. Reaction Pathways for the Thermal Decomposition of Methyl Butanoate. *J. Org. Chem.* **2013**, *78* (12), 5898–5908.

(12) Debnath, S.; Sengupta, A.; Raghavachari, K. Eliminating Systematic Errors in DFT via Connectivity-Based Hierarchy: Accurate Bond Dissociation Energies of Biodiesel Methyl Esters. *J. Phys. Chem. A* **2019**, *123* (16), 3543–3550.

(13) Drew, K. L. M.; Reynisson, J. The Impact of Carbon-Hydrogen Bond Dissociation Energies on the Prediction of the Cytochrome P450 Mediated Major Metabolic Site of Drug-like Compounds. *Eur. J. Med. Chem.* **2012**, *56*, 48–55.

(14) Sharp, T. R. Calculated Carbon-Hydrogen Bond Dissociation Enthalpies for Predicting Oxidative Susceptibility of Drug Substance Molecules. *Int. J. Pharm.* **2011**, *418* (2), 304–317.

(15) Reid, D. L.; Calvitt, C. J.; Zell, M. T.; Miller, K. G.; Kingsmill, C. A. Early Prediction of Pharmaceutical Oxidation Pathways by Computational Chemistry and Forced Degradation. *Pharm. Res.* **2004**, *21* (9), 1708–1717.

(16) Clayden, J.; Greeves, N.; Warren, S. *Organic Chemistry*; Oxford University Press, 2012.

(17) Huang, J. B.; Zeng, G. S.; Li, X. S.; Cheng, X. C.; Tong, H. Theoretical Studies on Bond Dissociation Enthalpies for Model Compounds of Typical Plastic Polymers. *IOP Conf. Ser. Earth Environ. Sci.* **2018**, *167*, 012029.

(18) Blanksby, S. J.; Ellison, G. B. Bond Dissociation Energies of Organic Molecules. *Acc. Chem. Res.* **2003**, *36* (4), 255–263.

(19) Berkowitz, J.; Ellison, G. B.; Gutman, D. Three Methods to Measure RH Bond Energies. *J. Phys. Chem.* **1994**, *98* (11), 2744–2765.

(20) Li, X.; Xu, X.; You, X.; Truhlar, D. G. Benchmark Calculations for Bond Dissociation Enthalpies of Unsaturated Methyl Esters and the Bond Dissociation Enthalpies of Methyl Linolenate. *J. Phys. Chem. A* **2016**, *120* (23), 4025–4036.

(21) Zhao, Y.; Truhlar, D. G. How Well Can New-Generation Density Functionals Describe the Energetics of Bond-Dissociation Reactions Producing Radicals? *J. Phys. Chem. A* **2008**, *112* (6), 1095–1099.

(22) Chan, B.; Radom, L. Hierarchy of Relative Bond Dissociation Enthalpies and Their Use to Efficiently Compute Accurate Absolute Bond Dissociation Enthalpies for C-H, C-C, and C-F Bonds. *J. Phys. Chem. A* **2013**, *117* (17), 3666–3675.

(23) Curtiss, L. A.; Redfern, P. C.; Raghavachari, K. Gaussian-4 Theory. *J. Chem. Phys.* **2007**, *126* (8), 084108.

(24) DeYonker, N. J.; Cundari, T. R.; Wilson, A. K. The Correlation Consistent Composite Approach (ccCA): An Alternative to the Gaussian-N Methods. *J. Chem. Phys.* **2006**, *124* (11), 114104.

(25) Hehre, W. J.; Ditchfield, R.; Radom, L.; Pople, J. A. Molecular Orbital Theory of the Electronic Structure of Organic Compounds. V. Molecular Theory of Bond Separation. *J. Am. Chem. Soc.* **1970**, *92* (16), 4796–4801.

(26) George, P.; Trachtman, M.; Bock, C. W.; Brett, A. M. An Alternative Approach to the Problem of Assessing Destabilization Energies (strain Energies) in Cyclic Hydrocarbons. *Tetrahedron* **1976**, *32* (3), 317–323.

(27) Wheeler, S. E.; Houk, K. N.; Schleyer, P. v. R.; Allen, W. D. A Hierarchy of Homodesmotic Reactions for Thermochemistry. **2009**. https://doi.org/10.1021/ja805843n.

(28) Ramabhadran, R. O.; Raghavachari, K. Theoretical Thermochemistry for Organic Molecules: Development of the Generalized Connectivity-Based Hierarchy. *J. Chem. Theory Comput.* **2011**, *7* (7), 2094–2103.

(29) Deshmukh, M. M.; Gadre, S. R. Molecular Tailoring Approach for the Estimation of Intramolecular Hydrogen Bond Energy. *Molecules* **2021**, *26* (10), 2928.

(30) Ramabhadran, R. O.; Sengupta, A.; Raghavachari, K. Application of the Generalized Connectivity-Based Hierarchy to Biomonomers: Enthalpies of Formation of Cysteine and Methionine. *J. Phys. Chem. A* **2013**, *117* (23), 4973–4980.

(31) Collins, E. M.; Sengupta, A.; AbuSalim, D. I.; Raghavachari, K. Accurate Thermochemistry for Organic Cations via Error Cancellation Using Connectivity-Based Hierarchy. *J. Phys. Chem. A* **2018**, *122* (6), 1807–1812.

(32) Maier, S.; Thapa, B.; Raghavachari, K. G4 Accuracy at DFT Cost: Unlocking Accurate Redox Potentials for Organic Molecules Using Systematic Error Cancellation. *Phys. Chem. Chem. Phys.* **2020**, *22* (8), 4439–4452.

(33) Frisch, Æ.; Frisch, M. J.; Clemente, F. R.; Trucks, G. W. *Gaussian 09 User's Reference*; 2009.

(34) *Gaussian 16 Rev. C.01/C.02 Release Notes*. https://gaussian.com/relnotes (accessed 2023-07-19).

(35) Lee, C.; Yang, W.; Parr, R. G. Development of the Colle-Salvetti Correlation-Energy Formula into a Functional of the Electron Density. *Phys. Rev. B Condens. Matter* **1988**, *37* (2), 785–789.

(36) Zhao, Y.; Truhlar, D. G. A New Local Density Functional for Main-Group Thermochemistry, Transition Metal Bonding, Thermochemical Kinetics, and Noncovalent Interactions. *J. Chem. Phys.* **2006**, *125* (19), 194101.

(37) Becke, A. D. A New Mixing of Hartree–Fock and Local Density‑functional Theories. *J. Chem. Phys.* **1993**, *98* (2), 1372–1377.

(38) Ernzerhof, M.; Scuseria, G. E. Assessment of the Perdew–Burke–Ernzerhof Exchange-Correlation Functional. *J. Chem. Phys.* **1999**, *110* (11), 5029–5036.

(39) Thapa, B.; Raghavachari, K. Accurate P Evaluations for Complex Bio-Organic Molecules in Aqueous Media. *J. Chem. Theory Comput.* **2019**, *15* (11), 6025–6035.

(40) Makam, P.; Yamijala, S. S. R. K. C.; Tao, K.; Shimon, L. J. W.; Eisenberg, D. S.; Sawaya, M. R.; Wong, B. M.; Gazit, E. Non-Proteinaceous Hydrolase Comprised of a Phenylalanine Metallo-Supramolecular Amyloid-like Structure. *Nat Catal* **2019**, *2* (11), 977–985.

(41) Kreitz, B.; Abeywardane, K.; Goldsmith, C. F. Linking Experimental and Thermochemistry of Adsorbates with a Generalized Thermochemical Hierarchy. *J. Chem. Theory Comput.* **2023**, *19* (13), 4149–4162.

(42) Yamijala, S. S. R. K.; Ali, Z. A.; Wong, B. M. Acceleration vs Accuracy: Influence of Basis Set Quality on the Mechanism and Dynamics Predicted by Ab Initio Molecular Dynamics. *J. Phys. Chem. C* **2019**. https://doi.org/10.1021/acs.jpcc.9b03554.

(43) Paultre, C.-B.; Mebel, A. M.; O'Shea, K. E. Computational Study of the Gas-Phase Thermal Degradation of Perfluoroalkyl Carboxylic Acids. *J. Phys. Chem. A* **2022**, *126* (46), 8753–8760.

(44) Melin, T. R. L.; Harell, P.; Ali, B.; Loganathan, N.; Wilson, A. K. Thermochemistry of per- and Polyfluoroalkyl Substances. *J. Comput. Chem.* **2023**, *44* (4), 570–580.

Table of Contents Graphic